

Multiscale characterizations of structural evolution in mesoporous CeO₂

Tianyu Li and Efrain E. Rodriguez*

Department of Chemistry and Biochemistry, University of Maryland,
College Park, Maryland 20742-2115, USA

Supplementary Information

1. Synthesis of mesoporous SBA-15 and Kit-6 Templated Mesoporous CeO₂

Mesoporous CeO₂ was synthesized via a nanocasting method similar to the previously reported approach¹⁻³.

Silica template KIT-6 and SBA-15 are used for the synthesis. The silica template SBA-15 and KIT-6 were first prepared via reported methods^{4,5}, for which 85 °C was used as the aging temperature during synthesis.

In a typical synthesis of KIT-6 mesoporous silica template, 8.0 g of P123 (EO₂₀PO₇₀EO₂₀) is first dissolved in 288 mL of distilled water 16 g of 35 wt % HCl solution. The mixture is stirred at room temperature until complete dissolution of P123. 8g of *N*-butanol is then added to the solution. After stirring for 1 h, 17 g of TEOS (tetraethoxysilicon) is added into the solution under the stirring. The mixture is left under vigorous stirring in a closed flask for 24 h at room temperature then aged at 85 °C for another 24 h (solution in a closed autoclave). The final product is filtered and washed with water and ethanol several times. The white powder is first

dried at 100 °C for 24 h and then calcinated at 550 °C for 24h under air to remove the surfactant.

In a typical synthesis of SBA-15 mesoporous silica template, 5.0 g of F127 ($\text{EO}_{106}\text{PO}_{70}\text{EO}_{106}$) is first dissolved in 240 mL of distilled water and 10.5 g of 35 wt % HCl solution. The mixture is stirred at room temperature until complete dissolution of F127. 24 g of *N*-butanol is then added to the solution. After stirring for 1 h, 16 g of TEOS is added into the solution under the stirring. The mixture is left under vigorous stirring in a closed flask for 24 h at room temperature then aged at 85 °C for another 24 h (solution in a closed autoclave). The final product is filtered and washed with water and ethanol several times. The white powder is first dried at 100 °C for 24 h and then calcinated at 550 °C for 24h under air to remove the surfactant.

In a typical synthesis of mesoporous CeO_2 , 0.5000g as-prepared mesoporous silica was initially dispersed in 20.0 mL 95% ethanol. Then 1.362g $\text{Ce}(\text{NO}_3)_3 \cdot 6\text{H}_2\text{O}$ was also dissolved in the same solution. The mixture was stirred at room temperature until all solvents evaporated and the mixture became a dry powder. The powder was later transferred to a glass vial (diameter ~ 5 mm) and under calcination at 560 °C for 6h (ramping rate 1°C/min). The calcination allows the conversion of $\text{Ce}(\text{NO}_3)_3 \cdot 6\text{H}_2\text{O}$ to pure CeO_2 . To fully remove the silica template, the CeO_2 /silica composite was soaked in 2M NaOH solution at 80 °C overnight; this step was repeated three times. After washing 3 times with distilled water and twice with ethanol, the final mesoporous CeO_2 product was dried in air at 80°C overnight and then at 150°C for an additional 24h.

Transmission electron microscopy (TEM)

Transmission electron microscopy (TEM) image was taken using JEOL JEM 2100 LaB6 TEM equipment.

In-situ USAXS/WAXS Experiment Setup

We performed synchrotron-based, in situ ultra-small-angle X-ray scattering (USAXS) and WAXS/XRD measurements at the USAXS facility at the Advanced Photon Source, Argonne National Laboratory, U.S.A. ⁶. We used monochromatic X-rays at 21 keV ($\lambda = 0.5904 \text{ \AA}$) in the study.

We used a Linkam 1500 thermal stage to control the temperature. Linkam 1500 thermal stage also allows for flowing different environmental gas. We use air as environment gas in our heating experiment.

To fix the mesoporous powder samples onto the vertical heating stage, we place a very thin layer of powder in between two transparent sapphire windows, the thickness of powder is measured to be $\sim 50 \mu\text{m}$, thin enough to allow the transmission of the X-ray. High temperature ceramic binder is then applied on the edge of the sapphire windows to hold the sandwich structure even at high temperatures (**Fig. S3a and S3b**). The prepared sample is loaded to the heating stage for the in-situ measurement (**Fig. S3c**). Sample-detector distance of USAXS characterization is calibrated with Silver Behenate standard. Sample- detector distance of WAXS is calibrated with LaB6 standard. The X-ray beam positions on the samples are determined via scanning the transmission profile of the sample film (optimized 60% transmission). The X-ray beam positions on the samples are determined each time starting a new experiment.

For the heating/cooling cycle experiment, a heating/cooling rate of $20 \text{ }^\circ\text{C /min}$ is used. Once the temperature reaches the characterization temperature (e.g. 100°C , 200°C), the temperature will hold until the USAXS/WAXS measurements at this temperature is complete.

The data acquisition times for USAXS and WAXS/XRD are 90 s and 30 s, respectively. In the heating to 1000 °C, data is collected every 100°C. In the cooling from 1000 °C, data is collected every 200°C. In the heating to 600 °C, data is collected every 50°C. In the cooling from 600 °C, data is collected every 100°C.

The collected USAXS patterns are reduced and fitted with Irena⁷. Rietveld refinement is performed on WAXS pattern with GSASII⁸.

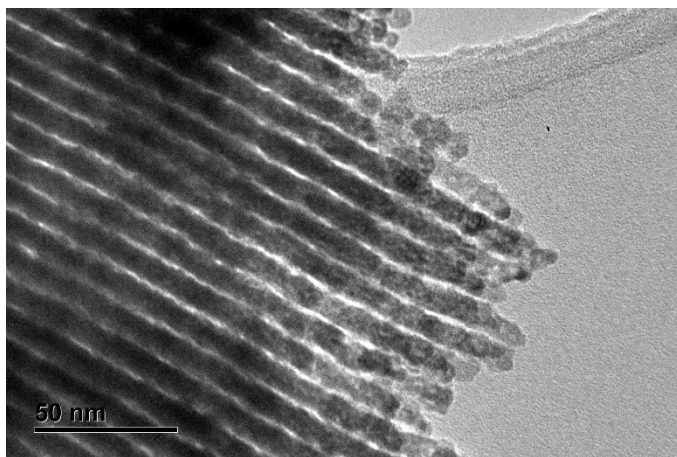


Fig S1. TEM of as synthesized SBA-15 templated mesoporous CeO_2 .

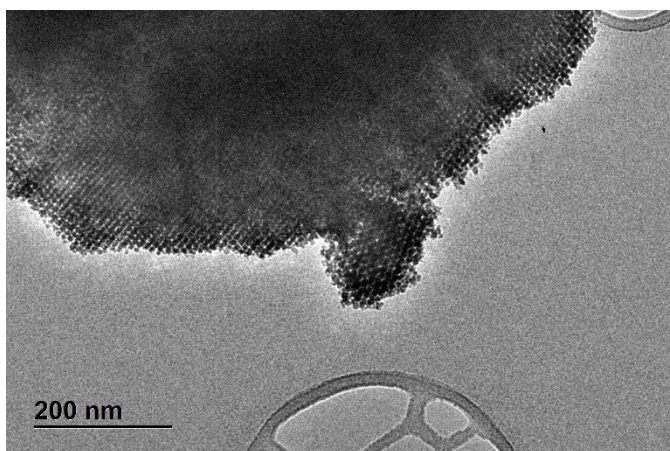


Fig S2. TEM of as synthesized KIT-6 templated mesoporous CeO_2 .

a)



b)



c)



Fig S3. a) and b) Mesoporous CeO₂ samples for the USAXS/WAXS experiment. The powder is in between two transparent sapphire windows. c) Linkam 1500 thermal stage.

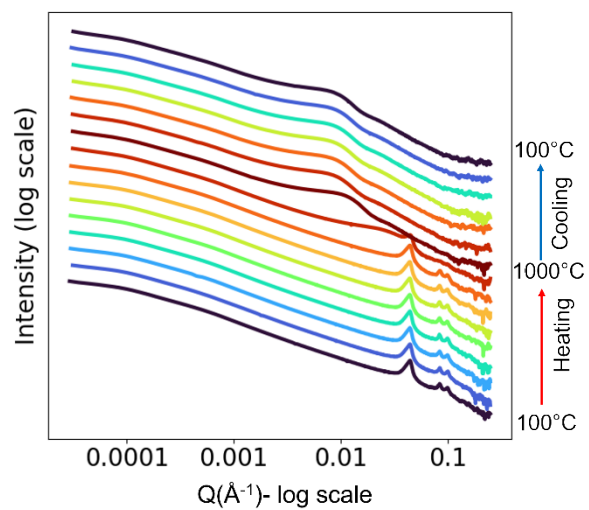


Fig S4. In-situ USAXS patterns of SBA-15 templated mesoporous CeO₂ under heating/cooling to/from 1000 °C.

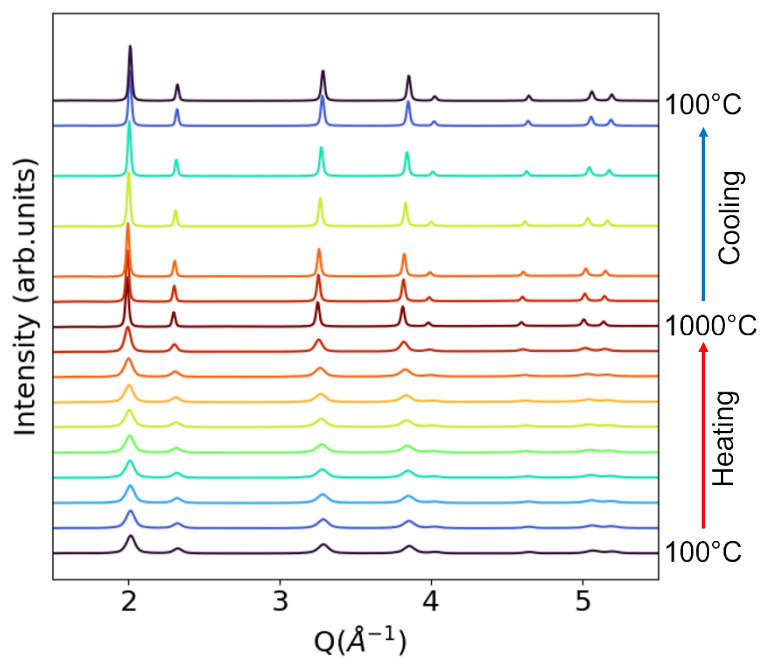


Fig S5. In-situ WAXS patterns SBA-15 templated mesoporous CeO₂ under heating/cooling to/from 1000 °C.

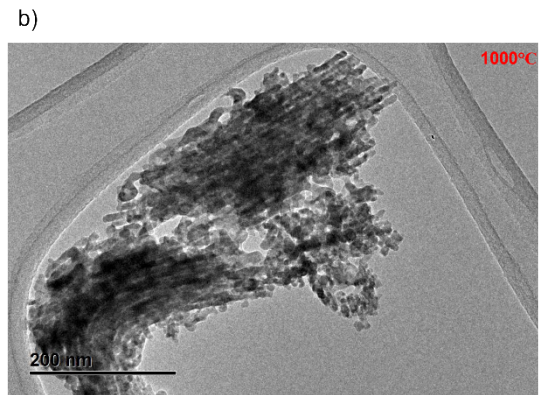
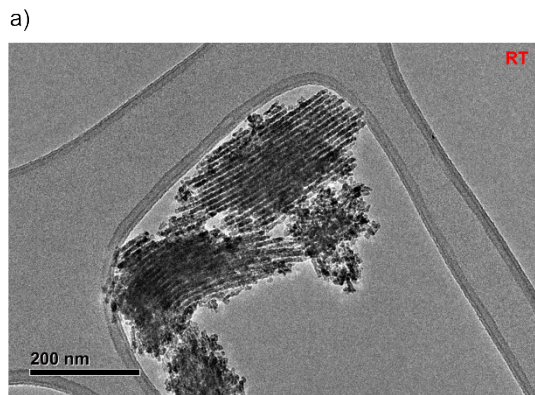


Fig S6. In-situ TEM of SBA-15 templated mesoporous CeO_2 at 25 °C (a) and 1000°C (b).

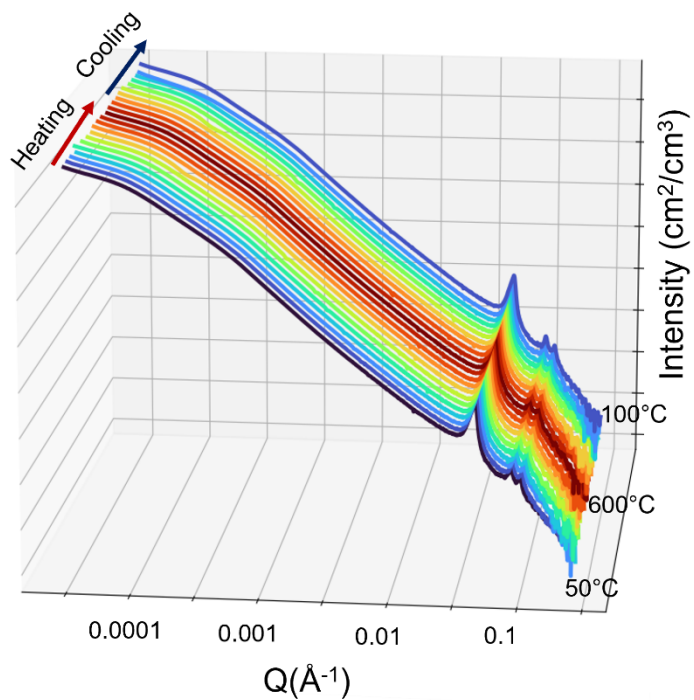


Fig S7. In-situ USAXS patterns of SBA-15 templated mesoporous CeO_2 under heating/cooling to/from 600°C .

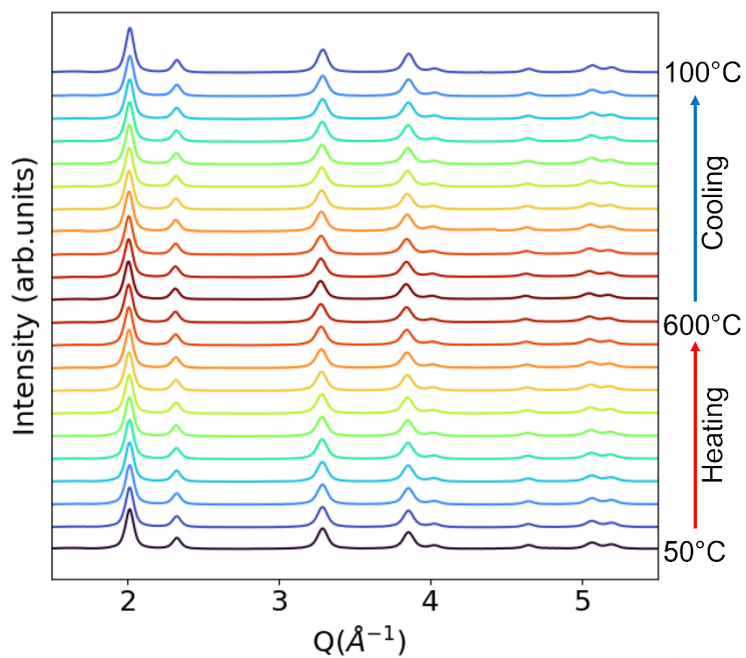


Fig S8. In-situ WAXS patterns SBA-15 templated mesoporous CeO_2 under heating/cooling to/from 600°C .

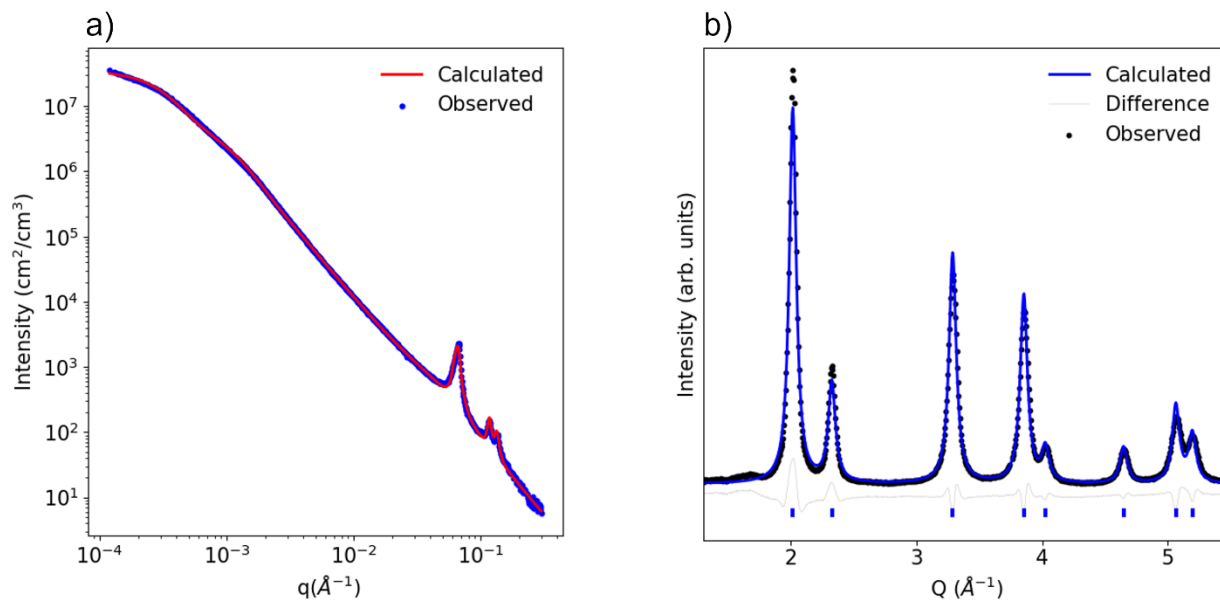


Fig S9. (a)USAXS data with fitting and (b) WAXS pattern with refinement of SBA-15 templated mesoporous CeO₂ at 50 °C.

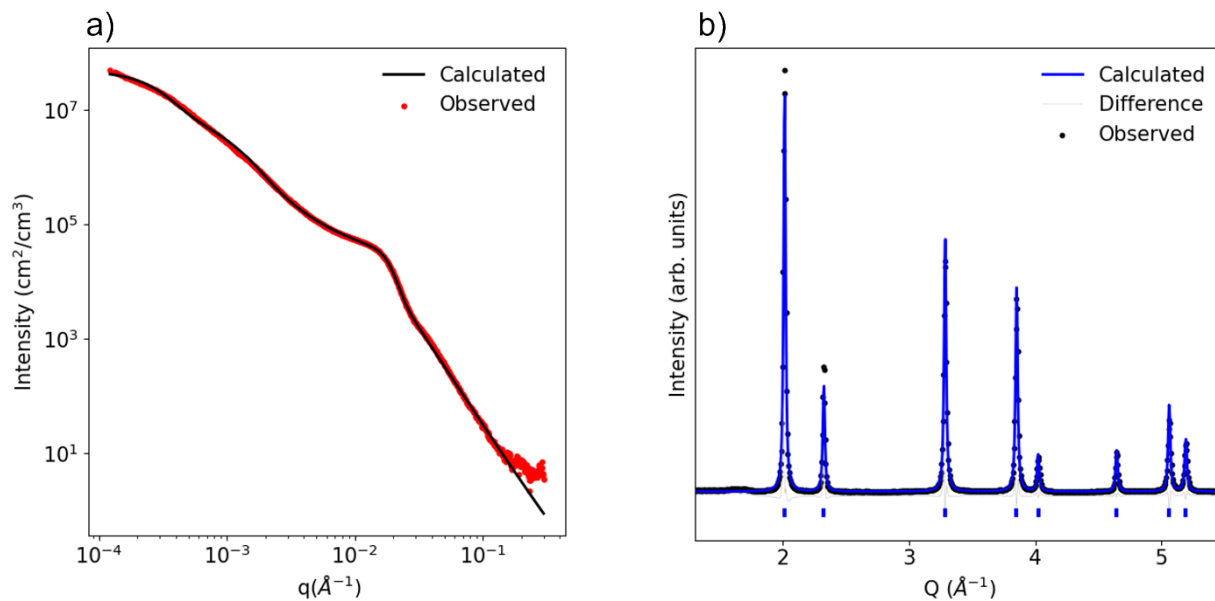


Fig S10. (a)USAXS data with fitting and (b) WAXS pattern with refinement of SBA-15 templated mesoporous CeO₂ at 1000 °C.

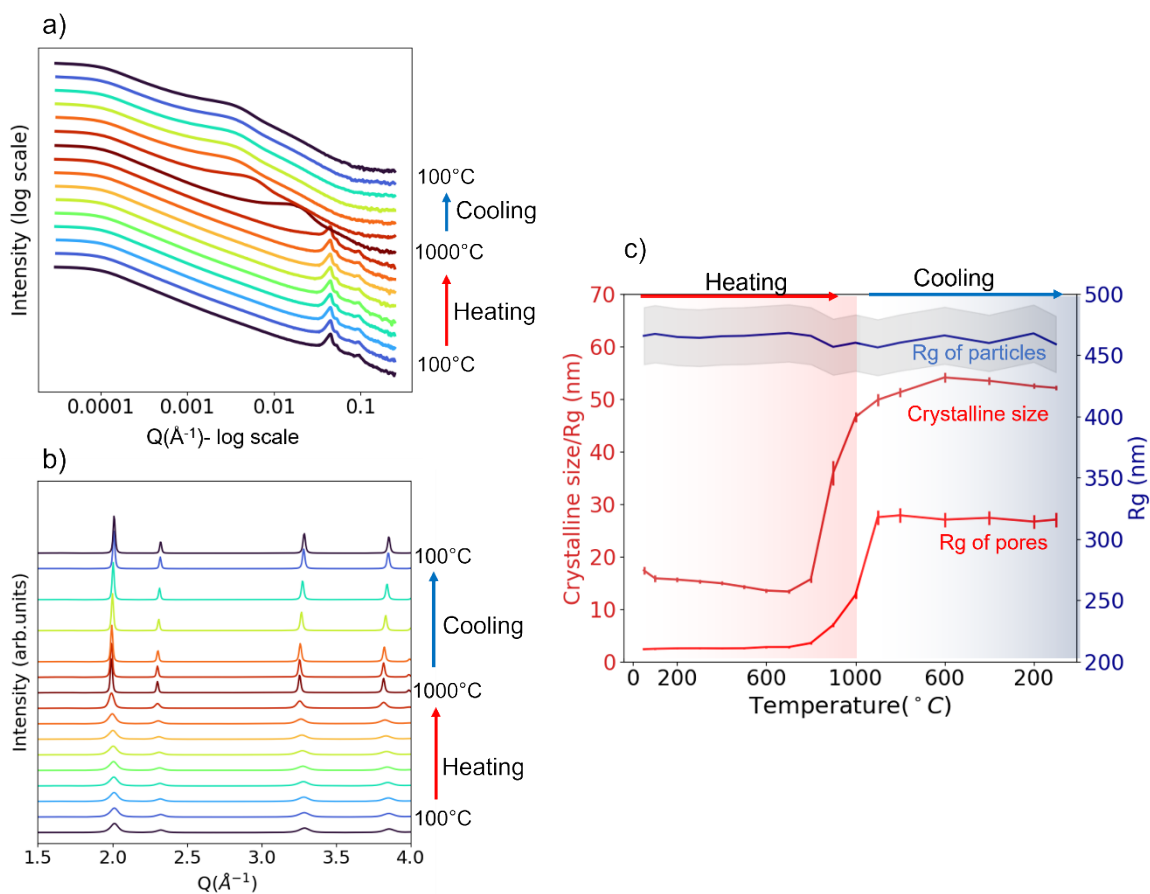


Fig S11. In-situ USAXS patterns (a) and WAXS patterns(b) under heating/cooling to/from 1000 °C. Extracted grain size, Rg of pores and Rg of particles under heating/cooling to/from 1000 °C (c). Data are collected for KIT-6 templated mesoporous CeO₂. USAXS data (a) is plotted at log scale for Q and intensity.

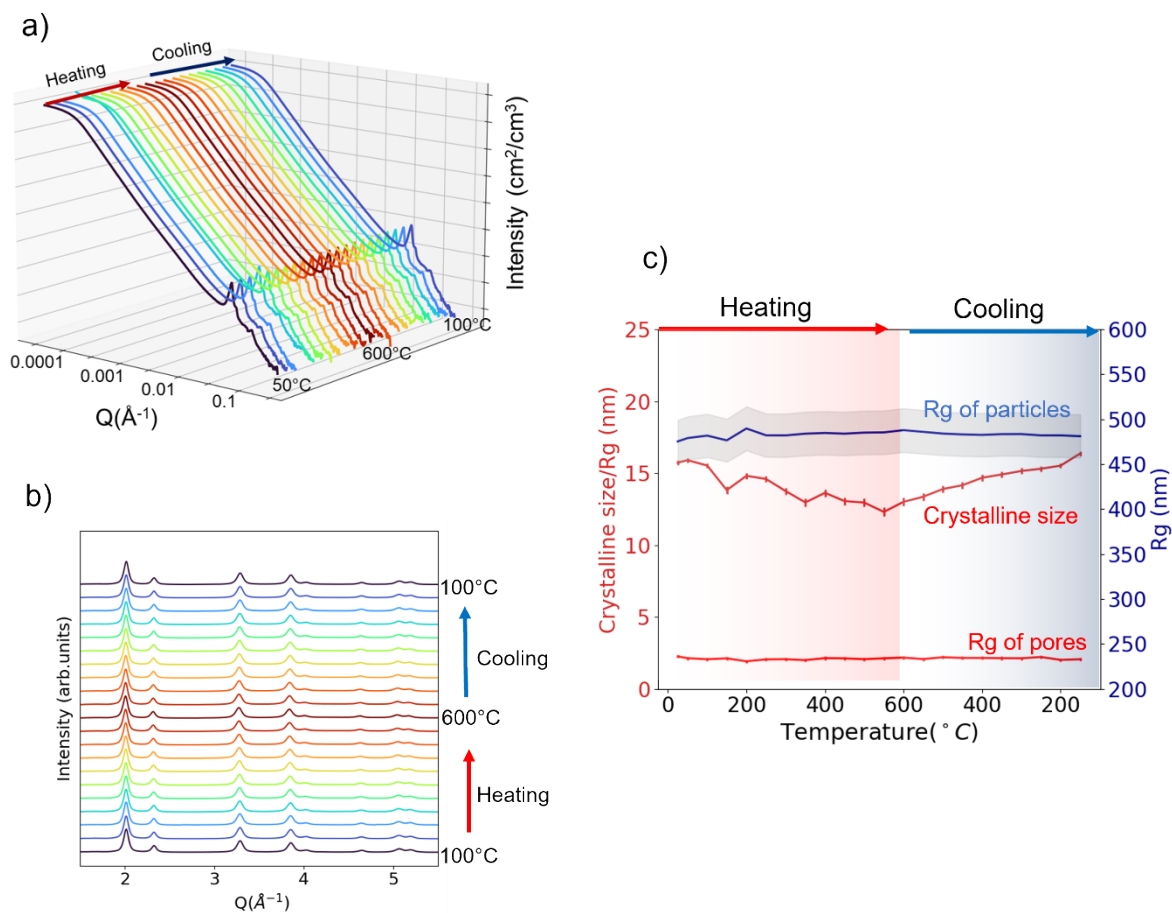


Fig S12. In-situ USAXS patterns (a) and WAXS patterns(b) under heating/cooling to/from 600 °C. Extracted grain size, Rg of pores and Rg of particles under heating/cooling to/from 600 °C (c). Data are collected for KIT-6 templated mesoporous CeO₂. USAXS data (a) is plotted at log scale for Q and intensity.

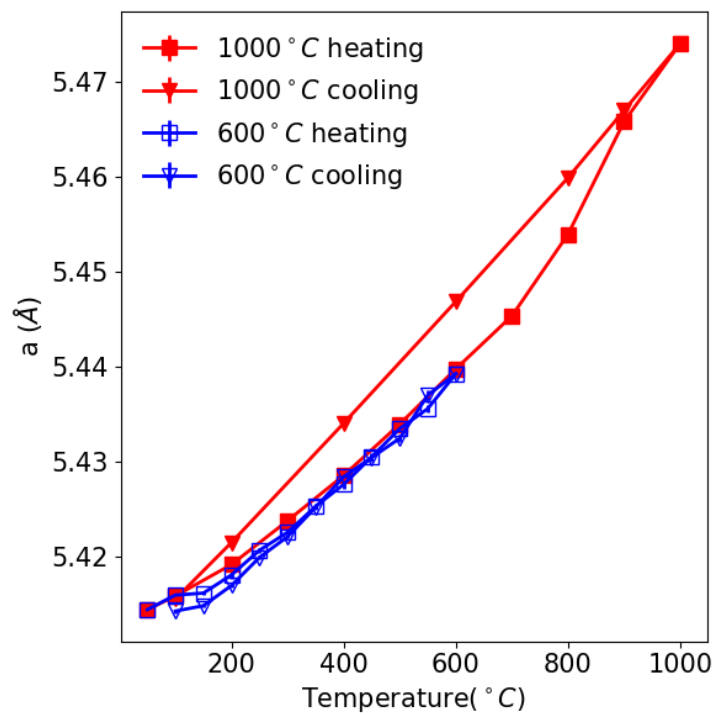


Fig S13. Lattice expansion under heating/cooling to/from 1000 °C and under heating/cooling to/from 600 °C for KIT-6 templated mesoporous CeO₂.

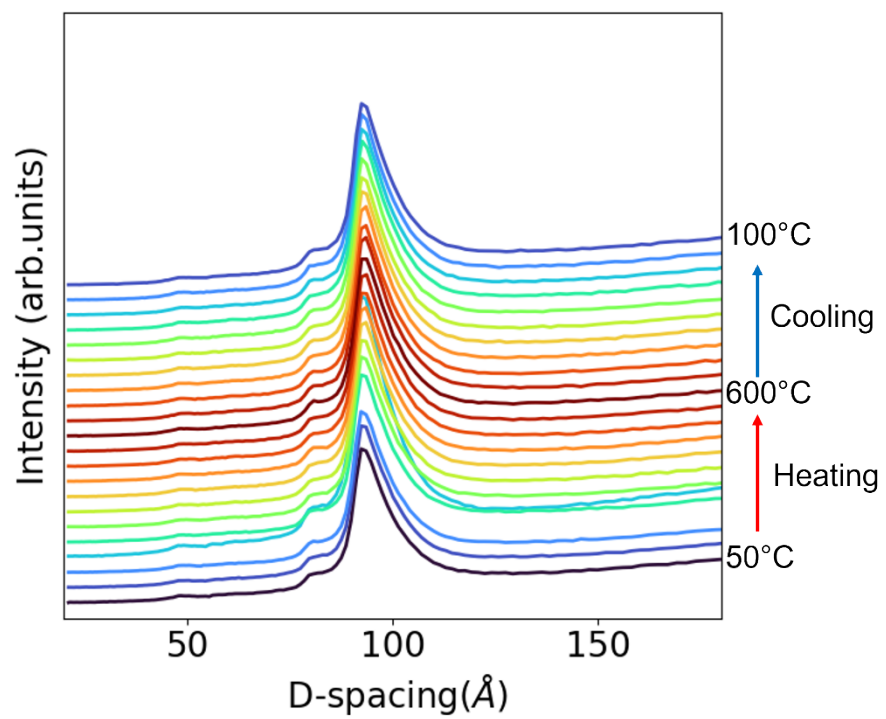


Fig S14. (211) Diffraction peak from the ordered mesopores under heating/cooling to/from 600 °C for KIT-6 templated mesoporous CeO₂.

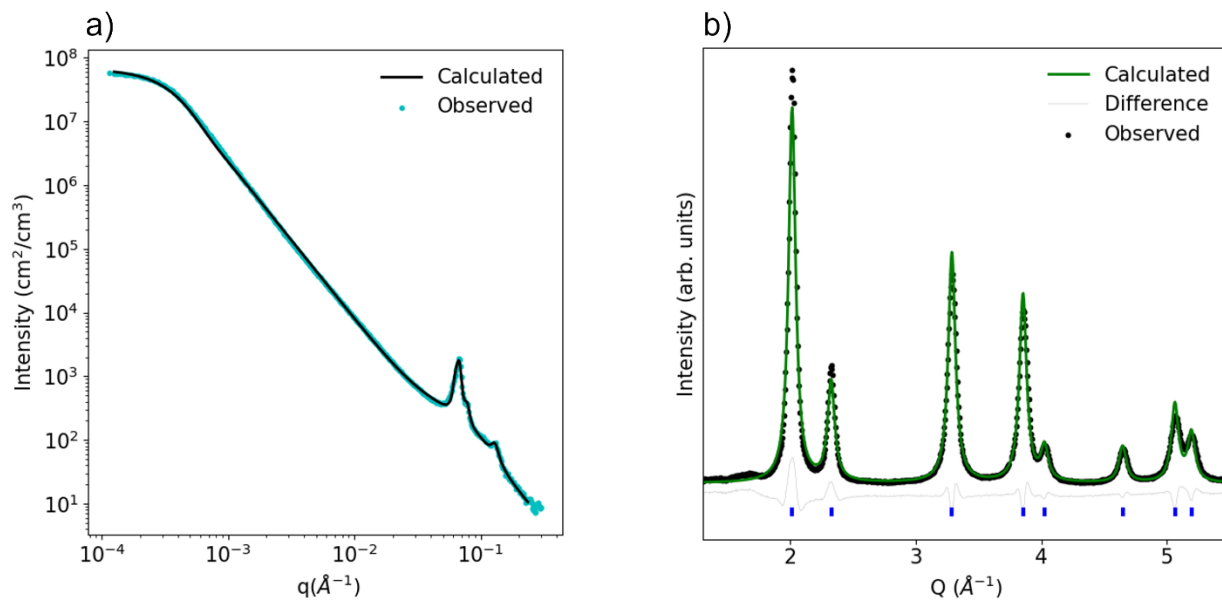


Fig S15. (a)USAXS data with fitting and (b) WAXS pattern with refinement of KIT-6 templated mesoporous CeO₂ at 50 °C.

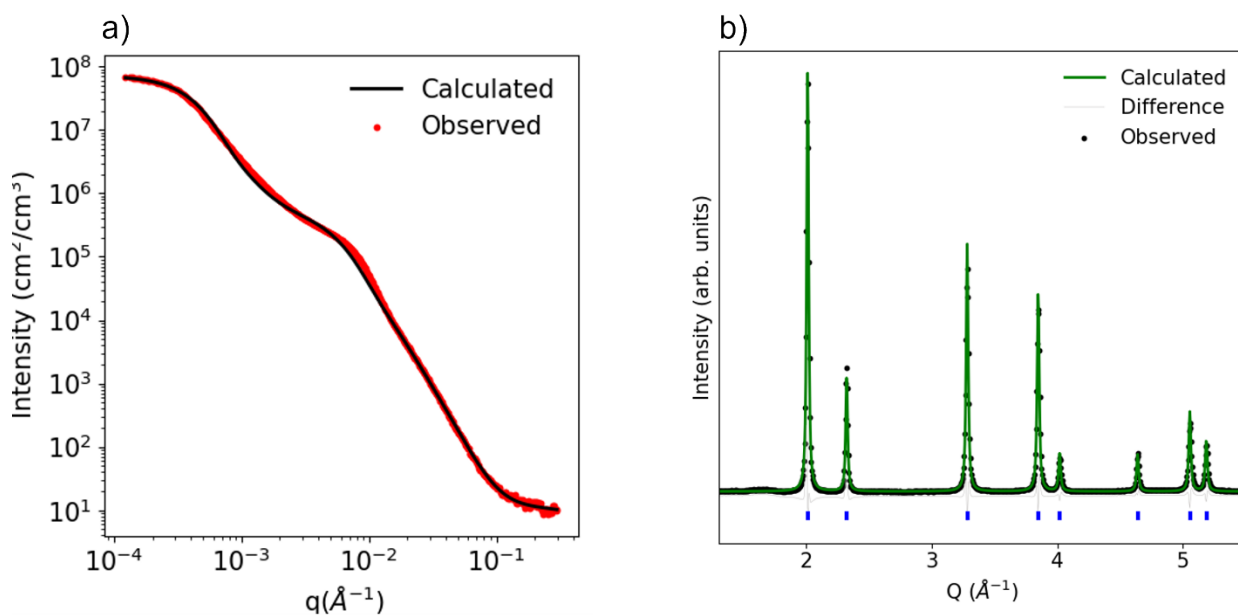


Fig S16. (a)USAXS data with fitting and (b) WAXS pattern with refinement of KIT-6 templated mesoporous CeO₂ at 1000 °C.

References:

- 1 S. C. Laha and R. Ryoo, *Chem. Commun.*, 2003, **3**, 2138–2139.
- 2 P. Ji, J. Zhang, F. Chen and M. Anpo, *J. Phys. Chem. C*, 2008, **112**, 17809–17813.
- 3 F. Kleitz, L. A. Solovyov, G. M. Anilkumar, S. H. Choi and R. Ryoo, *Chem. Commun.*, 2004, **4**, 1536–1537.
- 4 T.-W. Kim, F. Kleitz, B. Paul and R. Ryoo, *J. Am. Chem. Soc.*, 2005, **127**, 7601–7610.
- 5 D. Zhao, J. Feng, Q. Huo, N. Melosh, G. H. Fredrickson, B. F. Chmelka and G. D. Stucky, *Science (80-.)*, 1998, **279**, 548–552.
- 6 J. Ilavsky, F. Zhang, R. N. Andrews, I. Kuzmenko, P. R. Jemian, L. E. Levine and A. J. Allen, *J. Appl. Crystallogr.*, 2018, **51**, 867–882.
- 7 J. Ilavsky and P. R. Jemian, *J. Appl. Crystallogr.*, 2009, **42**, 347–353.
- 8 B. H. Toby and R. B. Von Dreele, *J. Appl. Crystallogr.*, 2013, **46**, 544–549.